

N 70 42233

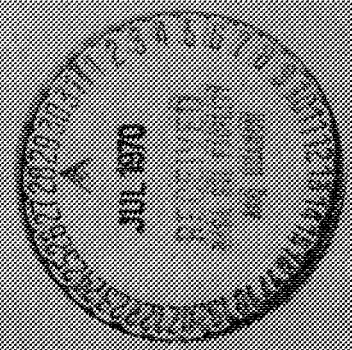
CR 110777

*Dr. John Edward
Case 2000
Lewis*

**DIVISION OF
FLUID, THERMAL AND AEROSPACE SCIENCES
SCHOOL OF ENGINEERING
CASE WESTERN RESERVE UNIVERSITY**

FLOW EXCURSIONS IN
A SIMULATED GAS-COOLED REACTOR PASSAGE
by
Paul Vingerhoet and Eli Reshotko

**CASE FILE
COPY**



UNIVERSITY CIRCLE • CLEVELAND, OHIO 44106

SOT 62156

FTAS/TR-68-34

FLOW EXCURSIONS IN
A SIMULATED GAS-COOLED REACTOR PASSAGE

by

Paul Vingerhoet and Eli Reshotko

September 1968

ABSTRACT

When a gas flows in a heated slender tube it exhibits the unusual characteristic of having two possible flow rates for a given pressure drop when the heat rate to the gas is constant. The lower flow rate is unstable and is associated with laminar flow while the larger flow rate is associated with turbulent flow and is considered stable.

These characteristics have been noted theoretically and have also to some extent been observed in the laboratory. The purpose of the present study is to experimentally study the characteristics of flow excursions believed to result from the laminar instability.

In the present work the steady-state characteristics of helium gas flowing in an electrically heated .094" ID Nichrome V tube 54" in length were observed and recorded. Constant pressure drop excursions were also triggered and observed and their time-histories are presented herein. The results tend to substantiate Reshotko's theory that an excursion is non-oscillatory and non-violent, and has a characteristic time proportional to the heat capacity of the tube, namely of the order of seconds to minutes.

ACKNOWLEDGMENTS

The authors wish to acknowledge the financial support of the National Aeronautics and Space Administration through Grant NGR-36-003-064.

TABLE OF CONTENTS

ABSTRACT	ii
ACKNOWLEDGEMENTS	iii
TABLE OF CONTENTS	iv
LIST OF FIGURES	vi
LIST OF SYMBOLS	vii
CHAPTER	Page
1. INTRODUCTION	1
1.1 Origin and General Discussion of the Problem	1
1.2 Purposes of Investigation	6
2. APPARATUS	8
2.1 Apparatus Design	8
2.2 General Arrangement and Instrumentation	8
3. STEADY-STATE OPERATION	10
3.1 One-Dimensional Flow Analysis	10
3.2 Steady-State Flow Characteristics	10
3.3 Test Procedure	12
3.4 Results	13

TABLE OF CONTENTS (continued)

	Page
4. EXCURSION STUDIES	16
4.1 Stability of One-Dimensional Flow With Constant Pressure Drop	16
4.2 Excursions at Constant Pressure Drop	17
4.3 Test Procedure	18
4.4 Results	19
5. CONCLUSIONS	23
APPENDIX A Harry's Steady State Analysis	25
APPENDIX B Reshotko's Stability and Excursion Analysis	31
REFERENCES	39

LIST OF FIGURES

Figure	Page
1. Cutaway Sketch of a Solid Core Nuclear Rocket Reactor	41
2. Flow Diagram of Experimental Apparatus	42
3. Photograph of Vacuum Tank and Associated Instrumentation	43
4. Instrumentation for Heating, Temperature and Δp Measurements	44
5. Theoretically Calculated Steady-State Characteristics	45
6. Experimentally Observed Steady-State Characteristics for Constant Electrical Heating	46
7. Calculated Heat Rate to the Gas for Constant Electrical Heating	47
8. Experimental Steady-State Characteristics for Constant Heat Rate to the Gas	48
9. Schematic of Excursion Path	49
10. Excursion Characteristics Calculated from Theoretically Predicted Steady-State Characteristics ($\bar{Q}_0 = \text{constant}$)	50
11. Excursion Characteristics Calculated from Experimentally Observed Steady-State Characteristics ($\bar{Q}_0 = \text{constant}$)	51
12. Excursion Characteristics Calculated from Experimentally Observed Steady-State Characteristics ($\bar{Q}_0 \neq \text{constant}$)	52
13. Experimentally Observed Excursion Characteristics	53
14. Possible Variation of \bar{Q}_0 During Excursion Experiment	54

LIST OF SYMBOLS

A	Cross-sectional flow area
a	Cross-sectional area of "reactor core" associated with single passage
C	Sonic velocity
c	Specific heat of "core" material
C_p	Specific heat at constant pressure
C_v	Specific heat at constant volume
d	Tube internal diameter
f	Fanning friction factor
g	Gravitational acceleration
h	Forced convection heat transfer coefficient
I	Current
L	Tube length
k	Thermal conductivity
m	Density of "reactor core" material
m	Exponent of viscosity variation with temperature, $\mu = \mu_0 T^m$
M	Mach number
n	Exponent of friction factor variation with Reynolds number, $f = f_0 / Re^n$
p	Pressure
Pr	Prandtl number
q	Heat rate per unit mass of fluid
q(x)	Normalized distribution of heat transfer to gas
Q	Heat rate per unit inside surface area of tube

LIST OF SYMBOLS (continued)

\bar{Q}	Average heat rate to gas per unit inside surface area of tube
R	Gas constant
Re	Reynolds number
r_h	Hydraulic radius ($r_h = d/4$ for round tubes)
T	Absolute temperature
τ	Dimensionless time unit
t	Time
u	Average velocity in axial direction
V	Voltage
W	Mass flow rate
x	Distance along the tube
γ	Ratio of specific heats, C_p/C_v
$\gamma(t)$	Defined as: $\gamma(t) = (A/m @ r_h)(\bar{h}/c)$
μ	Viscosity
ρ	Density
ϕ	Reactor energy release rate
τ	Final-to-initial gas temperature ratio

SUBSCRIPTS

o	Initial constant
0	Value at unstable equilibrium point
1	Conditions at entrance to the flow passage
L	Conditions at exit of the flow passage

LIST OF SYMBOLS (continued)

w	Conditions at wall
b	Evaluated at bulk conditions
f	Evaluated at film conditions
avg	Average
max	Maximum

1. INTRODUCTION

1.1 Origin and General Discussion of the Problem

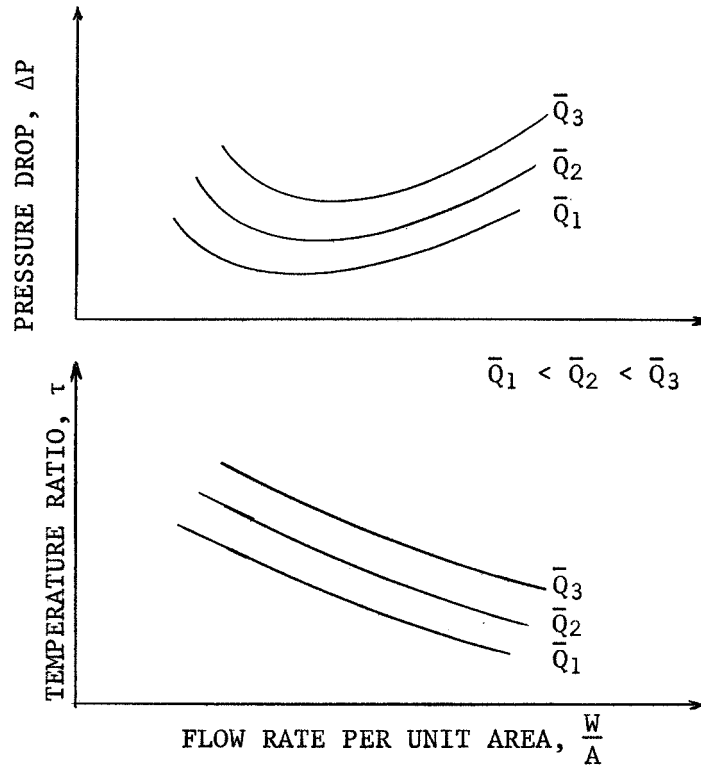
In the core of a nuclear rocket engine, the propellant, hydrogen gas, is heated in hundreds of parallel coolant passages to temperatures at core exit as high as 20-30 times those at core entrance (1). A typical solid core nuclear rocket of the type discussed herein is shown in Figure 1 depicting the coolant passages in a cutaway.

In such a reactor the static pressure drop across all the coolant passages is set by the pressure drop between the inlet and outlet plenums. It is conceivable that non-uniform flow distributions could exist among the flow passages, due either to dimensional differences or to non-uniform spatial heat generation rates, thus possibly inflicting a limit on the performance of such a nuclear propulsion system.

In the analysis of the steady flow of a gas in a tube with friction and heat addition (this model is applicable to high temperature ratio heat-exchangers as well as to nuclear rocket engines*) one finds some interesting peculiarities. At a constant heat rate to the gas the pressure drop versus flow rate curves are concave upward in the laminar-turbulent flow regime. This general shape indicates the existence of two possible flow rates for any given pressure drop at a constant heat rate to the gas.

* Even though only the nuclear rocket application is discussed herein, the results of this investigation are of interest in predicting the stability characteristics of high temperature ratio heat-exchangers.

Also, the outlet-to-inlet gas temperature ratio decreases monotonically with increasing flow rate in laminar-turbulent transition region. A representative set of steady-state characteristics are shown below,



where for any given flow rate the pressure drop increases with \bar{Q} as shown. The temperature ratio corresponding to the minimum pressure drop for any constant heat rate curve is termed the "critical" temperature ratio. For temperature ratios greater than critical the change of pressure drop with flow rate at constant heat rate to the gas is negative. This negative slope is associated with laminar flow. For temperature ratios less than critical the slope is positive and the flow is usually turbulent.

Much attention has been devoted to the left or laminar portion of the steady-state characteristic curves since this portion of the curve is believed to be unstable; in fact the instability has been coined a "laminar instability". As a result of this laminar instability spontaneous flow excursions to higher or lower flow rates are presumed to take place if one were to operate on the negatively sloped portion of a steady-state characteristic curve, assuming that the pressure drop is held constant.

One of the early analytical endeavors on the stability of gas flows in heated channels was by Longmire (2). Using a perturbation technique he showed that instabilities occur when the change in pressure drop with flow rate at constant heat rate to the gas is negative. He also showed that this condition occurs in steady, heated, laminar gas flows at low flow rates and so concluded that laminar gas flow in heated channels is unstable.

Bussard and DeLauer (3) used Longmire's result to show that turbulent flow is always stable and that laminar flows are unstable for large exit-to-entrance temperature ratios.

Guevara, McInteer and Potter (4) attempted to study laminar instabilities experimentally. They used helium gas flowing in an electrically heated capillary tube instrumented with appropriate thermal, and pressure regulating devices to measure the steady-state characteristics of the flow of gases in heated tubes. They found that when the apparatus was operated in the region of negative change in pressure drop with flow rate for constant electrical heating

spontaneous oscillations of the tubes' local temperatures resulted. For continuous changes in power input they also observed "discontinuous" changes in temperature.

Harry (5) calculated the stability limits of laminar instability for the nuclear rocket application. He did this by detailed numerical integration of the flow of para-hydrogen in long tubes of small circular cross-section. He found that the minimum pressure drop at constant heat input occurs just below the flow rate where the tube exit condition becomes laminar, and that laminar instabilities are potentially a problem at low pressures whenever the wall-to-fluid-inlet temperature ratio is high.

Gruber and Hyman (6) calculated stability limits and flow sensitivity factors for fully-developed laminar gas flows.

Bankston (7) experimentally determined stability limits of gaseous hydrogen flow in a tube and presented graphs of pressure drop versus flow rate for constant heat input to the gas for several different test sections.

Turney, Smith and Juhasz (8) conducted an experiment to determine the steady-state pressure drop characteristics of normal hydrogen gas flowing in an electrically heated test section in the laminar-turbulent flow regime. Their results show that in the steady-state a heated channel may have two different flow rates for the same pressure drop at constant heat rate to the gas. Their results agree reasonably well with theory. They also show that for outlet-to-inlet fluid temperature ratios greater than 5.5 the change of pressure drop

with flow rate is negative for a constant heat rate to the gas.

Kolbe (9) in an experimental program was also able to verify the existence of two flow rates for a given pressure drop and heat rate to the gas.

More recently, Reshotko (10) completed a time-dependent analysis to determine the nature of the "laminar instability" problem, including effects of heat exchange between the gas and the core of a nuclear rocket engine. He confirmed the existence of an instability when the change in pressure drop with flow rate is negative for a constant heat rate to the gas. For the case he considered, Reshotko concludes that,

"...the instability is not in any way hydrodynamic. Rather, it is associated with the compatibility between the heat-transfer characteristics of the flow passage and the thermal characteristic of the core".

He further concludes that there is nothing violent about the instability, since the characteristic time is not infinitesimal, but is of the order of seconds to minutes, and that there is no oscillatory behavior, but rather a steady procession away from the steady equilibrium point during a flow excursion.

Applying this theory to the flow passages of a nuclear rocket one assumes ideally that there is no radial heat generation between any two flow passages and that the behavior of one passage does not affect the pressure difference between the inlet and outlet plenums maintained by the other passages. Thus it is conceivable, if the reactor were to operate in the laminar regime, that local perturbations in reactor heat generation might cause flow excursions.

Excursions to lower flow rates cause tube burnout, whereas excursions to higher flow rates consume excessive amounts of propellant.

In order to avoid this unstable region, nuclear rocket engines are normally designed to operate in the region where the flow in the coolant passages is completely turbulent, i.e., where the change in pressure drop with weight flow at constant heat rate to the gas is positive. However, during start-up and shut-down the reactor must operate, at least temporarily, in the unstable region. The problem of instability is not as serious during start-up because of the short time involved in passing through the laminar-turbulent regime. However during shut-down, particularly after long periods of operation at high power levels, the reactor decay heat may be sufficiently large to require cooling of the core assembly for relatively long periods of time. During this time it is reasonable to assume that a flow excursion could take place in an errant tube when this tube experiences laminar or transitional flow between the fixed pressure boundaries of the inlet and outlet plenums.

1.2 Purposes of Investigation

The purposes of this investigation are: first, to obtain as extensive a set as possible of steady-state operating data for a single flow passage; and second, to experimentally trigger and observe an excursion at constant pressure drop from an unstable laminar equilibrium point on the negatively sloped portion of a steady-state characteristic curve to the corresponding stable turbulent equilibrium point on the positively sloped portion of the same steady-state

characteristic curve. The experimental results will in each case be compared with theoretical predictions. Excursions to lower flow rates will not be discussed herein.

2. APPARATUS

2.1 Apparatus Design

The experimental apparatus used in the present investigation was designed and constructed by Kolbe (9). The test section was specifically designed to simulate a nuclear reactor flow passage and instrumented to observe the steady-state flow characteristics of helium gas in the laminar-turbulent regime at low pressures.

2.2 General Arrangement and Instrumentation

A schematic drawing of the test apparatus is shown in Figure 2. The test section is made of Nichrome V (80% nickel, 20% chromium) and is 4.5 feet long, 0.094 inches I.D., and has a wall thickness of 0.020 inches. Nichrome V was chosen because of the small variation of its resistivity with temperature (11). The test section is suspended between the inlet and outlet plenums by a spring suspension system to allow for thermal expansion when the test section is electrically heated by a variac regulated A.C. source. A liquid nitrogen heat exchanger is used to obtain a constant gas temperature at the entrance of 140°R.

A pressure regulator regulates the inlet pressure from a high pressure reservoir to a constant inlet pressure of 1 psig. A second pressure regulator between the high and low pressure reservoirs controls and maintains a constant pressure drop across the test section. The differential pressure across the test section is measured by a transducer. All other pressures are measured using pressure gauges.

The inlet and outlet gas temperatures are measured by a copper-constantan and a shielded chromel-alumel thermocouple respectively. Five thermocouples mounted on the tube wall also measure tube wall temperatures at five arbitrary points.

A rotameter is placed in the line just before the inlet plenum to measure the flow rate.

To get an idea of the limits of the apparatus, at a constant inlet pressure of 1 psig, pressure drops of up to 5 psi and electrical heating inputs of up to 96.4 watts may be imposed.

The whole system is in a closed loop. The test section and the inlet and outlet plenums are confined in a vacuum tank to try and eliminate heat losses by convection.

Photographs of the apparatus and recording instruments are shown in Figures 3 and 4 respectively.

3. STEADY-STATE OPERATION

3.1 One-Dimensional Flow Analysis

An approximate solution to the steady one-dimensional flow of a perfect gas in a constant-area flow passage with friction and heat addition was obtained by Harry (5) and is shown in Appendix A. Harry's result for the case of uniform heat addition is equation (A.1.14),

$$P_{avg} \Delta p = \frac{RT_1}{g} \left(\frac{W}{A} \right)^2 \left[(\tau - 1) + \frac{f_o \mu_1^{n_L}}{2r_h \left[4r_h \left(\frac{W}{A} \right) \right]^n} \frac{1}{(mn + 2)} \frac{\tau^{mn + 2} - 1}{(\tau - 1)} \right] \quad (3.1.1)$$

The first term in the square brackets represents the momentum pressure drop while the second term represents the frictional pressure drop. At low flow rates the frictional pressure drop dominates and at high flow rates the momentum pressure drop dominates.

3.2 Steady-State Flow Characteristics

In the present investigation helium gas enters the flow passage at liquid nitrogen temperature (140°R). The steady-state characteristics were calculated using equation (3.1.1). For laminar flow $f_o = 16$, $n = 1$, $m = 0.65$, and for turbulent flow $f_o = 0.046$, $n = 0.2$, $m = 0.65$. The results of these calculations are shown in Figure 5

for a number of gas heating rates.* Remember that in the steady-state all the heat, Q , goes into heating the gas. The appropriate equation (eq. A.1.10) can be rewritten as,

$$\left(\frac{W}{A}\right) C_p (T_2 - T_1) = Q \left(\frac{L}{r_h}\right)$$

or in terms of the temperature ratio, τ

$$\left(\frac{W}{A}\right) C_p (\tau - 1) = Q \left(\frac{L}{r_h T_1}\right)$$

Figure 5 shows that the pressure drop versus flow rate curves for constant heat rate to the gas are concave upward. This indicates the existence of two flow rates for any constant pressure drop. The temperature ratio is inversely proportional to the flow rate at a constant heat input to the gas as indicated in Figure 5.

According to Harry (5) the flow is arbitrarily chosen as laminar up to a Reynolds number of 2100 and turbulent down to a Reynolds number of 1000, where the Reynolds number is evaluated at the film temperature, $[T_f = (T_w + T_b)/2]$. In this investigation the same criterion was employed except that the Reynolds number was evaluated at the bulk gas temperature. Turney, Smith, and Juhasz (8) substantiate, by experiment, that this procedure yields reasonable results.

* The properties of helium used herein are those of reference 12.

3.3 Test Procedure

Before any data were taken the whole helium loop and vacuum chamber surrounding the test section were purged to the atmosphere. They were then evacuated to a vacuum of approximately 0.01 torr. The vacuum chamber was then sealed off from the helium loop by closing a shut-off valve connecting the two. The helium loop was then filled with helium gas from a high pressure storage tank to a pressure of 18 psig. The liquid nitrogen was then allowed to flow through the heat exchanger. The helium circulating pump and electrical heating were then turned on. The inlet pressure was adjusted to 1 psig. The pressure drop (independent variable) was controlled by the pressure regulator downstream of the test section while the flow rate (dependent variable) was read at any time through a glass tube in its construction.

The system was assumed to be in steady-state when all of the indicators were reading constant values.

The steady-state characteristics relating pressure drop and temperature ratio with flow rate for various electrical heating rates are shown in Figure 6. These data were obtained for a given electrical heating rate by increasing the pressure drop, using the downstream pressure regulator, from approximately .25 to 4.0 psi. The pressure drop was increased in increments. After each increase it took several minutes to reach steady-state conditions. When steady-state conditions prevailed the appropriate measurements were taken.

The constant electrical heating curves in Figure 6 were reproducible to within approximately 7%, thus giving a certain degree of confidence in the results of the experiment.

By calculating the average heat rate to the gas, \bar{Q} , using the equation $\bar{Q} = \left(\frac{W}{A}\right) C_p (T_{out} - T_{in})$ it was found that \bar{Q} varied significantly along curves of constant electrical heat input as seen by Figure 7. Ideally (in the steady-state solution) all electrical heating should go into heating the gas. Therefore, it was concluded that there were considerable heat leaks to the test section. The heat leaks were such that even at zero electrical heating there was substantial heating of the gas. An analysis of the heat losses was attempted by Kolbe (Appendix C, Reference 9), but not all of the heat losses could be accounted for satisfactorily.

Nevertheless it was still possible to generate the steady-state characteristics for constant \bar{Q} by connecting points of equal \bar{Q} on each of the curves of constant electrical heating. These curves are shown in Figure 8. In the same manner the temperature ratios for constant \bar{Q} were also plotted in Figure 8.

Using the technique just described it was possible to obtain the steady-state operating characteristics as described in Section 3.2.

3.4 Results

In comparing the theoretically calculated steady-state results of Figure 5 with the experimental results of Figure 8, the degree of agreement depends significantly on whether the flow is laminar or turbulent. In the turbulent region the pressure drop is in agreement

to within approximately 10%. In the laminar region, however, the experimentally observed pressure drop tends to be as much as 56% greater than predicted using equation (3.1.1). The agreement is better for higher flow rates and poorer for lower flow rates.

One might explain this rather poor agreement with theory in the following manner. In the laminar region the frictional pressure drop dominates in the equation for pressure drop. Since the frictional pressure drop is a strong function of viscosity, thus temperature, better agreement would have been established if the viscosity had been evaluated at the film temperature. Better agreement would have also followed if the friction factor had accounted for the radial temperature gradient. Turney, Smith and Juhasz (7) accounted for these effects and also the pressure losses due to entrance and exit geometry. By numerically computing the pressure losses in successive segments of their test section they achieved theoretical results which agreed with experiment to within 10%. Their apparatus was of similar construction to that of the present investigation except that they used normal hydrogen gas as the test fluid and measured the wall temperature every few inches.

In the turbulent flow region the dominant pressure drop is that of the momentum change and the effects just mentioned above have negligible contribution to the pressure loss.

Remember also that equation (3.1.1) is only an approximate solution for estimating the pressure drop.

It might also be mentioned here that in trying to operate the apparatus at low pressure drops, spontaneous oscillations in pressure

drop, flow rate, and temperatures were sometimes observed. It is thought by the author that these oscillations were in no way related to the instabilities or flow excursions of the kind discussed herein. Rather, they are thought to be a result of some mechanical instability related to the construction of the apparatus (there were considerable vibrations in parts of the helium loop caused by the vibrations of the circulating pump). By manually increasing the pressure drop to a point where the oscillations ceased and after several attempts at slowly decreasing the pressure drop, the low pressure drop operating points could be satisfactorily obtained in steady operation.

4. EXCURSION STUDIES

4.1 Stability of One-Dimensional Flow With Constant Pressure Drop

A time-dependent stability analysis was performed by Reshotko (10) using a perturbation technique. This analysis is presented in Appendix B. His results affirm the commonly accepted criterion that flows of the type discussed herein are subject to instabilities when the change in pressure drop with weight flow at constant heat rate to the gas is negative. He shows with equation (B.1.4) that instabilities may occur when

$$\left[\frac{\partial(\Delta p)}{\partial\left(\frac{W}{A}\right)} \right]_{\bar{Q}} < 0$$

He concludes that,

"...the instability is not in any way hydrodynamic. Rather it is associated with the compatibility between the heat-transfer characteristics of the flow passage and the thermal characteristic of the core."

Reshotko physically explains the instability and flow excursions at constant pressure drop as follows: if a flow passage were being operated at an equilibrium point on the left leg of the U-shaped characteristic curves shown in Figure 8, an excursion at constant pressure drop to a higher flow rate would require additional heat to the gas. This heat would be provided by further cooling of the core

and the excursion would continue; in an excursion from the same equilibrium point to a lower flow rate at constant pressure drop the gas requires less heat. Thus the additional heat goes into heating the core. Therefore, one concludes that the left or laminar leg is unstable since unbounded excursions at constant pressure drop may occur. For completeness excursions at constant pressure drop are now examined for the right leg. Operating on an equilibrium point on the right leg an excursion to higher flow rate at constant pressure drop would require a decrease in the heat rate to the gas and since the core is being cooled by this increase in flow rate there is an increase in the heating rate to the gas and the flow is driven back to the equilibrium point. An excursion at constant pressure drop to lower flow rate requires an increase in the heat rate to the gas and to the core, but since the heat generation rate of the reactor is constant the flow reverts back to the equilibrium point. Therefore, the higher flow rate equilibrium point is stable.

4.2 Excursion at Constant Pressure Drop

The analysis of an excursion at constant pressure drop was done by Reshotko (10) and is also presented in Appendix B. The time for an excursion is given in dimensionless time units, T , that are related to physical time by equation (B.2.2) as,

$$T = \frac{1}{m} \frac{A}{Q_{r_h}} \left(\frac{h_1}{c} \right)_0 t \quad (4.2.1)$$

While the steady-state flow and heat transfer characteristics of a flow passage are dependent solely on the fluid and internal geometry of the flow passage, the time for an excursion is related to the heat capacity of the core as shown in equation (4.2.1).

The time in dimensionless time units for an excursion to higher flow rate at constant pressure drop is given by equation (B.2.1) as,

$$T = \int_{\tau_i}^{\tau} \frac{\frac{d\bar{Q}}{d\tau} \left\{ 1 + XY - (1 - n) \frac{d \ln \left(\frac{W}{A} \right)}{d \ln \bar{Q}} \right\} \Big|_{\Delta P}}{\frac{h_1}{(h_1)_0} \left[\frac{\tau^{mn} + 1}{(\tau - 1)(mn + 1)} - 1 \right] \left[\bar{Q}_0 - \bar{Q} \right]} d\tau \quad (4.2.2)$$

where X and Y are defined in section B.2.

Equation (4.2.2) can be evaluated numerically from any set of steady-state operating curves. For example, in this investigation equation (4.2.2) was solved for both the steady-state characteristics shown in Figures 5 and 8. The excursion characteristics of Figure 5 are shown in Figure 10 and those of Figure 8 are shown in Figures 11 and 12.

4.3 Test Procedure

All flow excursions were run at a constant pressure drop of 1 psi. The constant heating curve of $\bar{Q} = 0.376 \text{ BTU/sec-ft}^2$ was chosen as the steady-state heating curve on which to base the excursions.

Therefore as seen in Figure 9 the excursion would run from $\bar{Q}_0 = 0.376$

(IV = 96.4 watts, $\frac{W}{A} = 1.17 \text{ lbm/sec-ft}^2$) to $\bar{Q} = .376$ (IV = 0 watts, $\frac{W}{A} = 2.90 \text{ lbm/sec-ft}^2$) at a constant pressure drop of 1 psi.

The excursion was initiated by operating on the unstable equilibrium point on the left leg of the steady-state operating curve at $\bar{Q}_0 = .376 \text{ Btu/sec-ft}^2$, $\Delta p = 1 \text{ psi}$. The electrical heating was then shut off to trigger the excursion. During the excursion the pressure drop and inlet pressure were manually adjusted to maintain constant values of 1 psi and 1 psig respectively. The gas exit temperature and flow rate measurements were recorded at successive time intervals. The time-history results of such an excursion are shown in Figure 13.

4.4 Results

Looking at Figure 10 one sees that the general shape of an excursion curve (i.e., the time-history of \bar{Q}) is described as follows: a gradual increase in \bar{Q} as the excursion first proceeds away from the unstable equilibrium point; a rapid increase; a maximum; a rapid decrease followed by a gradual decrease in \bar{Q} to its final stable equilibrium point corresponding to the original value of \bar{Q} . Since the shape and duration of the initial increase in \bar{Q} is directly dependent on the means and magnitude of the initial perturbation, the most meaningful way of comparing theory with experiment is perhaps to compare the time it takes to go from 1/2 maximum (1/2 rise), approaching \bar{Q}_{\max} , to 1/2 maximum (1/2 fall), leaving \bar{Q}_{\max} :

In the calculation of the excursion characteristics from equation 4.2.2 one must know the value of \bar{Q}_0 . In analyzing a nuclear reactor flow passage \bar{Q}_0 is equal to the heat rate to the gas at the initial

unstable equilibrium point and from equation (B.1.3),

$$\bar{\phi}_0 \alpha x_h / A = \bar{Q}_0$$

thus \bar{Q}_0 is constant during an excursion since $\bar{\phi}_0$ is constant. Since it was impossible to keep $\bar{\phi}_0$ (the equivalent of reactor energy release rate) constant during an excursion on the present apparatus, a lower limit of \bar{Q}_0 was established as that value of \bar{Q} which corresponded to the zero electric power input corresponding to the appropriate flow rate (Figure 8). Thus an upper limit of $\bar{Q}_0 = \text{constant}$ and a lower limit of $\bar{Q}_0 \neq \text{constant}$ ($\bar{Q}_0 =$ the corresponding zero electric power heat rate value) were established for the present calculations of excursion times. The actual time for an excursion would be expected to fall somewhere in between these upper and lower limits. A sketch indicating the upper and lower limits of \bar{Q}_0 is shown in Figure 14.

The characteristic time was found from equation (4.2.1) to be 19.3 seconds, (i.e. $1T = 19.3 \text{ sec}$). This characteristic time is the same for all the excursions observed since the same initial unstable equilibrium point was used for all excursions.

The excursion results using equation (4.2.2) on the theoretical steady-state characteristics of Figure 5 are shown in Figure 10. The corresponding experimentally observed excursion characteristics are shown in Figure 13. Only the upper limit, $\bar{Q}_0 = \text{constant}$, is shown for this case since the characteristic curves were obtained completely by theoretical means. The time from 1/2 rise to 1/2 fall was $19T$ for

theory and $4.1T$ for experiment. This difference indicates that the completely theoretically calculated excursion time is much too high. This poor agreement is understandable since the steady-state characteristics of Figure 5 are in error by as much as 56% as mentioned in section 3.4.

Applying equation (4.2.2) to the experimentally observed steady-state characteristics of Figure 8 yields the results shown in Figures 11 and 12 for $\bar{Q}_0 = \text{constant}$ (upper limit) and $\bar{Q}_0 \neq \text{constant}$ (lower limit) respectively. The corresponding experimentally observed excursion characteristics are those of Figure 13.

In comparing theory (Figures 11 and 12) and experiment (Figure 13) one notices a discrepancy in the values of \bar{Q}_{max} . The theoretical curves are however based on the steady-state data of Figure 8 which are reproducible only to about 7%. Hence the value of \bar{Q}_{max} of Figure 13 is within expectations. The excursion times are compared between $\bar{Q} = 0.450 \text{ Btu/ft}^2\text{-sec}$ on the way up and $\bar{Q} = 0.450 \text{ Btu/ft}^2\text{-sec}$ on the way down. One finds that for $\bar{Q}_0 = \text{constant}$ equation (4.2.2) predicts an excursion time from "1/2 rise to 1/2 fall" (at $\bar{Q} = 0.450$) of $6T$, 30% above the experimental value of $4.7T$. For $\bar{Q}_0 \neq \text{constant}$ theory predicts $3.5T$, 28% below experiment.

The experimentally observed excursion time would be expected to lie somewhere between the upper and lower limits presented herein. Thus the agreement of theory with experiment is certainly reasonable.

Not only does equation (4.2.2) predict excursion times reasonably well, but the experiment tends to support the notion that an excursion

is non-violent in nature. Rather it is a steady procession away from an unstable equilibrium point. The experiment also supports the notion that an excursion is non-oscillatory in nature and that the characteristic time is intimately connected with the heat capacity of the core.

As an added degree of confidence in the experimental observations, the excursion data were reproducible to within approximately 5%.

5. CONCLUSIONS

In the present investigation steady-state operating characteristics have been obtained experimentally for laminar, transitional and turbulent flow of a gas in a heated tube. Excursions from an unstable laminar equilibrium point to a stable turbulent equilibrium point at constant pressure drop were triggered and observed. It was shown that the time-history of an excursion is directly related to the heat capacity of the core, and that an excursion is non-violent and non-oscillatory in nature.

During an excursion the gas is heated and the heat rate to the gas reaches a maximum at a flow rate just larger than that for a neutral disturbance. The characteristic times were observed to be of the order of seconds to minutes and the excursion was seen to be a steady procession away from an unstable laminar equilibrium point to a stable turbulent equilibrium point. This nature supports the theory of Reshotko (10). It also tends to support the notion that with the aid of feedback mechanisms a nuclear rocket might be operated in the "unstable" region.

It is also concluded that one might operate a reactor core in the "unstable" region for extended periods of time if there were built in means such that the pressure drop versus flow rate curves, for constant heat generation, are monotonic. This might even lead to better efficiencies, since very high exit temperature levels (limited only by core material limitations) may be obtained coupled with relatively low propellant consumption rates, whereas operating in the stable

region one must be content to have a high propellant consumption, low exit temperature nuclear rocket.

No conclusions can be drawn in this investigation concerning the mechanism of triggering an excursion in an actual reactor. In order for the excursions to occur at constant pressure drop in the present apparatus the excursion had to be "forced" to proceed from the unstable equilibrium point to the stable equilibrium point by shutting off the electrical heating and constantly adjusting the pressure drop to remain constant. Conversely, in a nuclear rocket the pressure drop between the plenums would always remain constant while a single errant passage might experience a flow excursion due to some disturbance. Nevertheless, the characteristics of such an excursion are presented herein.

APPENDIX A

HARRY'S STEADY STATE ANALYSIS

A.1 One-Dimensional Steady-State Equation

The assumptions in Harry's analysis of a gas flowing in a heated channel (5) are the following:

- a. Perfect gas relationship

$$p = \rho RT$$

- b. Constant area tube

- c. Very low Mach numbers

$$M \ll 1$$

- d. The friction factor is approximated as a function of Reynolds number

$$f = \frac{f_0}{Re^n}$$

- e. The viscosity is assumed a function of temperature

$$\mu(T) = \mu_0 T^m$$

- f. Constant heat input distribution along the tube

$$Q(x) = Q_0$$

The equations to be solved are:

Continuity

$$\frac{d}{dx} (\rho Au) = 0 \quad (\text{A.1.1})$$

Momentum

$$\frac{1}{\rho} \frac{dp}{dx} + \frac{u}{g} \frac{du}{dx} + \frac{f}{r_h} \frac{u^2}{2g} = 0 \quad (\text{A.1.2})$$

Energy

$$\frac{q}{u} dx + \frac{f}{r_h} \frac{u^2}{2g} dx = C_p dT - \frac{1}{\rho} dp \quad (\text{A.1.3})$$

State

$$p = \rho RT \quad (\text{A.1.4})$$

where q , the power per unit mass, is related to Q , the power per unit of surface area, by the relation

$$Q = \rho q r_h \quad (\text{A.1.5})$$

Using assumption (a) equation (A.1.1) becomes

$$\frac{du}{u} + \frac{d\rho}{\rho} = 0 \quad (\text{A.1.6})$$

The equation of state can be put into differential form as

$$\frac{dp}{p} = \frac{dT}{T} + \frac{d\rho}{\rho} \quad (\text{A.1.7})$$

Substituting equations (A.1.6) and (A.1.7) into (A.1.2) gives

$$\frac{dp}{\rho} - \frac{u^2}{g} \frac{dp}{p} + \frac{u^2}{g} \frac{dT}{T} + \frac{f}{2r_h} \frac{u^2}{g} dx = 0$$

Now, substituting (A.1.5) into (A.1.3) yields

$$\left(\frac{Q}{\rho u r_h} + \frac{f}{2r_h} \frac{u^2}{g} \right) dx = C_p dT - \frac{dp}{\rho}$$

If dT is eliminated and $p = \rho RT$ is substituted into the last two equations collecting terms gives

$$\left(1 - \frac{u^2}{gRT} + \frac{u^2}{gTC_p} \right) \frac{dp}{\rho} + \frac{u^2}{gTC_p} \frac{Qdx}{\rho u r_h} + \left(1 + \frac{u^2}{gTC_p} \right) \frac{f}{2r_h} \frac{u^2}{g} dx = 0 \quad (\text{A.1.8})$$

Using the sonic relations

$$C^2 = \gamma g R T$$

$$M^2 = \frac{u^2}{C^2}$$

one can show that

$$\frac{u^2}{gRT} = \gamma M^2$$

$$\frac{u^2}{gTC_p} = \frac{u^2 \gamma R}{\gamma gRTC_p} = (\gamma - 1)M^2 \quad (\text{A.1.9})$$

Since for the steady-state all the heat input goes into heating the gas, utilizing assumption (c) one can say

$$WC_p dT = Q \frac{A dx}{r_h} \quad (\text{A.1.10})$$

where A is the cross-sectional area of the tube.

Substituting equations (A.1.9) and (A.1.10) into (A.1.8) after multiplying through by $p \rho = \rho \cdot \rho R T$ and dropping terms of order M^2 yields

$$p dp + \frac{R}{g} \left(\frac{W}{A}\right)^2 \left(dT + \frac{f}{2r_h} T dx\right) = 0$$

Integrating this equation along the flow passage gives

$$\frac{p_2^2 - p_1^2}{2} + \frac{R}{g} \left(\frac{W}{A}\right)^2 \left[T_2 - T_1 + \frac{1}{2r_h} \int_{x=0}^x f T dx \right] = 0 \quad (\text{A.1.11})$$

Now, using assumptions (e) and (d)

$$\mu(T) = \mu_o T^m$$

$$f(x) = \frac{f_o}{Re^n} = \frac{f_o \mu^n}{\left[4r_h \left(\frac{W}{A}\right)\right]^n}$$

equation (A.1.11) becomes

$$P_{avg} \Delta P = \frac{R}{g} \left(\frac{W}{A}\right)^2 \left\{ T_2 - T_1 + \frac{1}{2r_h} \frac{f_o \mu_o^n}{\left[4r_h \left(\frac{W}{A}\right)\right]^n} \int_{x=0}^x T^{mn+1} dx \right\} \quad (A.1.12)$$

where P_{avg} is the arithmetic average of the inlet and outlet pressures.

Utilizing assumption (f) and integrating equation (A.1.10) along the tube yields

$$T = T_1 + \frac{Q_o x}{r_h \left(\frac{W}{A}\right) C_p} \quad (A.1.13)$$

Defining the temperature ratio as

$$\tau = \frac{T_2}{T_1}$$

one can substitute the temperature ratio and equation (A.1.13) into (A.1.12) and integrating to the end of the tube gives

$$p_{avg} \Delta p = \frac{RT_1}{g} \left(\frac{W}{A} \right)^2 \left[(\tau - 1) + \frac{f \mu_1^{n_L}}{2r_h \left[4r_h \left(\frac{W}{A} \right) \right]^n} \frac{1}{(mn + 2)} \frac{\tau^{mn + 2} - 1}{(\tau - 1)} \right]$$

(A.1.14)

APPENDIX B

RESHOTKO'S STABILITY AND EXCURSION ANALYSIS

B.1 Stability of One-Dimensional Flow With Constant Pressure Drop

The average heat rate to the gas, \bar{Q} used in this transient analysis is equivalent to the heat rate, Q , used in Harry's (5) steady-state analysis. Here \bar{Q} is defined as

$$\bar{Q} \equiv \frac{1}{L} \int_0^L Q(x,t) dx$$

The assumptions used in Reshotko's analysis (10) are:

- a. The flow is adequately described by one-dimensional relations that include heat addition and friction.
- b. Hydrodynamic instabilities of the nature associated with nonuniform velocity and temperature profiles are unimportant.
- c. The thermal response time of the core is the characteristic time for this problem since it is very large compared to the time for an acoustic disturbance to travel the length of the tube. The thermal response time of the core is also large compared to the residence time.
- d. The specific heat of the reactor coolant gas is constant, but the specific heat of the core may vary with temperature.

- e. The core temperature, $T_W(x, t)$, does not vary in a direction perpendicular to the flow direction, thus radial conduction is neglected.
- f. The axial conduction term is small compared to the other terms in the core energy equation.
- g. The average nuclear heat release, $\bar{\phi}$, is assumed constant.
- h. The friction factor is approximated as a function of the Reynolds number as

$$f = \frac{f_0}{Re^n}$$

- i. The heat flux, Q , has the same axial distribution as the reactor heat release, ϕ .
- j. The viscosity is assumed to vary with temperature as

$$\mu(T) = \mu_0 T^m$$

- k. The gas inlet temperature, T_1 , is constant.

The equations to be solved are grouped as follows: the gas equations; the core energy equation; the equation for heat transfer between the core and the gas. The procedure followed is to formulate the equations governing the integral properties of the tube flow. Some integral properties are mass flow, pressure drop, temperature ratio, average heat rate to the gas, and some characteristic wall temperature. The equations are then studied for their response to

a small disturbance about an equilibrium point.

"The time-dependent terms in the flow equations become negligibly small and only the time-dependent term in the equation governing the energy balance of the core is retained. The one-dimensional transient flow in the tubes may thus be regarded as a continuous succession of steady-state flows governed only by those terms appearing in the steady-state flow equations" (10).

The equations governing the gas are:

CONTINUITY

The continuity equation is nothing more than a statement that the mass flow per unit area, $\frac{W}{A}$, is constant over the length of the coolant passage, but can be a function of time.

MOMENTUM

For any passage whose steady-state operation is known (for example Figure 8) the momentum relation is available in "integral" form as

$$\Delta p = \Delta p \left(\frac{W}{A}, \bar{Q} \right)$$

ENERGY

$$\frac{W}{A} (t) C_p \int_0^L \frac{\partial T(x,t)}{\partial x} dx = \frac{1}{r_h} \int_0^L Q(x,t) dx$$

The equation governing the core is:

$$c(T_W) \frac{\partial T_W(x,t)}{\partial t} = \frac{\phi(x,t)}{m} - \frac{Q(x,t)A}{m \rho r_h}$$

The equation coupling the core with the gas is:

$$Q(x,t) = h(x,t) [T_w(x,t) - T(x,t)]$$

Solving these equations gives one equation governing the transient behavior of a reactor passage and that portion of the core associated with it. When put in the form appropriate to an excursion at constant Δp , this equation is

$$\alpha(t) \frac{d\bar{Q}}{dt} = \gamma(t) \left[\frac{\bar{\phi} \alpha r_h}{A} - \bar{Q} \right] \quad (\text{B.1.1})$$

where

$$\alpha(t) = \left\{ 1 + (\tau - 1) \left[\frac{\bar{h} \bar{T}_1}{\bar{Q}} \frac{d \left(\frac{\bar{T}}{\bar{T}_1} \right)}{d\tau} - \frac{\partial \widetilde{\ln h}}{\partial \tau} \right] \left[1 - \frac{d \ln \left(\frac{W}{A} \right)}{d \ln \bar{Q}} \Big|_{\Delta p} \right] - \frac{\partial \widetilde{\ln h}}{\partial \ln \left(\frac{W}{A} \right)} \frac{d \ln \left(\frac{W}{A} \right)}{d \ln \bar{Q}} \Big|_{\Delta p} \right\}$$

and,

$$\gamma(t) = \frac{A}{\pi \alpha r_h} \left(\frac{\bar{h}}{c} \right)$$

$$\bar{h} \equiv h_1 \left(\frac{\bar{T}}{T_1} \right)^{mn}$$

$$\frac{\bar{T}}{T_1} \equiv \left[\frac{1}{L} \int_0^L \left(\frac{T}{T_1} \right)^{mn+1} dx \right]^{1/(mn+1)}$$

$$\widetilde{\ln h} = \frac{1}{L} \int_0^L q(x) \ln h \, dx$$

$$\left(\frac{\bar{h}}{c} \right) = \frac{h_1}{c} \left[\frac{\tau^{mn+1} - 1}{(\tau - 1)(mn + 1)} \right]$$

$$\bar{\phi} \equiv \frac{1}{L} \int_0^L \phi \, dx$$

where $q(x)$ is a normalized distribution and is equal to unity for uniform heating.

To simulate a small perturbation about an equilibrium point let,

$$\begin{aligned} \bar{Q} &= \bar{Q}_0 + \bar{Q}_1 & \alpha &= \alpha_0 + \alpha_1 \\ \bar{\gamma} &= \bar{\gamma}_0 + \bar{\gamma}_1 & \bar{\phi} &= \bar{\phi}_0 \end{aligned} \tag{B.1.2}$$

where $(\quad)_1 \ll (\quad)_0$. Substituting equations (B.1.2) into equation (B.1.1) yields

Zero Order:

$$\bar{\phi}_0 a_{r_h}/A = \bar{Q}_0 \quad (\text{B.1.3})$$

First Order:

$$\alpha_0 \frac{d\bar{Q}_1}{dt} = -\gamma_0 \bar{Q}_1$$

The zero order solution is the equilibrium condition where all the reactor heat release goes into heating the gas.

Examining the first order solution by letting \bar{Q}_1 vary as $e^{\beta t}$ yields the growth rate given by β as

$$\beta = -\left(\frac{\gamma_0}{\alpha_0}\right)$$

Therefore, when β is negative the equilibrium condition is restored. When β is positive an instability is indicated. Examining β one sees that for,

$$\left(\frac{\bar{h}}{\bar{Q}}\right) \left[\frac{d\left(\frac{\bar{T}}{\bar{T}_1}\right)}{d\tau} \right] > \frac{\partial \ln h}{\partial \tau}$$

a condition that is just about always true, instabilities can occur

when,

$$\left[\frac{\partial \left(\frac{\Delta p}{W} \right)}{\partial \left(\frac{W}{A} \right)} \right]_{\bar{Q}} < 0 \quad (\text{B.1.4})$$

Therefore, equation (B.1.4) is the criterion for instability.

"Physically, the instability is not in any way hydrodynamic. Rather, it is a consequence of the compatibility between the heat-transfer characteristics of the flow passage and the thermal characteristic of the core (10)."

B.2 Excursions At Constant Pressure Drop

To initiate an excursion at constant pressure drop a small initial displacement of \bar{Q} , from its unstable equilibrium value of \bar{Q}_0 , along a line of constant pressure drop in a direction corresponding to an increase in flow rate is applied. The excursion then continues at constant pressure drop until the high-flow-rate stable equilibrium point is reached.

The equation describing a complete flow excursion at constant pressure drop is equation (B.1.1). The integration is carried out more conveniently in terms of temperature ratio, τ , which decreases monotonically during an excursion rather than \bar{Q} which first increases then decreases. The integral to be evaluated for an excursion to higher flow rate at constant pressure drop is,

$$T = \int_{\tau_i}^{\tau} \frac{d\bar{Q}}{d\tau} \left\{ 1 + XY - (1-n) \frac{d \ln \left(\frac{W}{A} \right)}{d \ln \bar{Q}} \Big|_{\Delta p} \right\} \frac{d\tau}{\frac{h_1}{(h_1)_0} \left[\frac{\tau^{mn+1} - 1}{(\tau-1)(mn+1)} \right] [\bar{Q}_0 - \bar{Q}]} \quad (\text{B.2.1})$$

where

$$X \equiv \left[\frac{h_1 T_i}{\bar{Q}} \left(\frac{(mn+2)(\tau-1)\tau^{mn+1} - (\tau^{mn+2} - 1)}{(mn+1)(mn+2)(\tau-1)} \right) - mn \left(1 - \frac{\ln \tau}{\tau-1} \right) \right]$$

$$Y \equiv \left[1 - \frac{d \ln \left(\frac{W}{A} \right)}{d \ln \bar{Q}} \Big|_{\Delta p} \right]$$

and, T is a dimensionless time defined as

$$T \equiv \frac{1}{m} \frac{A}{a r_h} \left(\frac{h_1}{c^t} \right)_0 t \quad (\text{B.2.2})$$

where h_1 is the heat transfer coefficient evaluated at the entrance temperature. For laminar flow $h_1 = 4.36 k / (4 r_h)$ and for turbulent flow $h_1 = \left(\frac{W}{A} \right)^{1-n} C_p f_o \mu_1^n / [2 (4 r_h)^n P_r^{2/3}]$.

REFERENCES

1. Spence, R. W.; and Durham, F. P.: The Los Alamos Nuclear Rocket Program. Astronautics and Aeronautics, June, 1965.
2. Longmire, Conrad: Stability of Viscous Flow Heat Exchanger, Unpublished work done at Los Alamos Scientific Laboratory, July 11, 1955.
3. Bussard, R. W.; and DeLaer, R. D.: Fundamentals of Nuclear Flight. McGraw-Hill Book Company, 1965.
4. Guevara, F. A.; McInteer, B. B.; Potter, R. M.: Temperature-Flow Stability Experiments. Los Alamos Scientific Laboratory. LAMS-2934, 1963.
5. Harry, David P., III: A Steady-State Analysis of the "Laminar-Instability" Problem Due to Heating Para-Hydrogen in Long, Slender Tubes. NASA TN D-2084, 1964.
6. Gruber, A. R.; and Hyman, S. C.: Flow Distribution Among Parallel Heated Channels. Am. Inst. Chem. Eng. J. 2, 1965.
7. Bankston, Charles A.: Fluid Friction, Heat Transfer, Turbulence, and Interchannel Flow Stability in the Transition from Turbulent to Laminar Flow in Tubes. Sc. D., The University of New Mexico, 1965.
8. Turney, George E.; Smith, John M.; and Juhasz, Albert J.: Steady-State Investigation of Laminar-Flow Instability Problem Resulting from Relatively Large Increases in Temperature of Normal Hydrogen Gas Flowing in Small Diameter Heated Tube. NASA TN D-3347, 1966.
9. Kolbe, E. R.: Apparatus for the Investigation of Instabilities in Gas-Cooled Heat Exchanger Tubes. Case Institute of Technology, Fluid Thermal and Aerospace Sciences TR-66-13, November, 1966.
10. Reshotko, E.: An Analysis of the "Laminar Instability" Problem in Gas-Cooled Nuclear Reactor Passages. AIAA Journal, Vol. 5, No. 9, September, 1967.
11. Technical Catalog NCR-58, Driver-Harris Company, Harrison, New Jersey.

12. Simmons, J. T.: The Physical and Thermodynamic Properties of Helium. William R. Whittaker Company Limited Technical Report D-9027, 1957.
13. Ellerbrock, H. H.; Livingood, J. N. B.; and Straight, D. M.: Fluid-Flow and Heat-Transfer Problems in Nuclear Rockets. NASA SP-20, December, 1962.

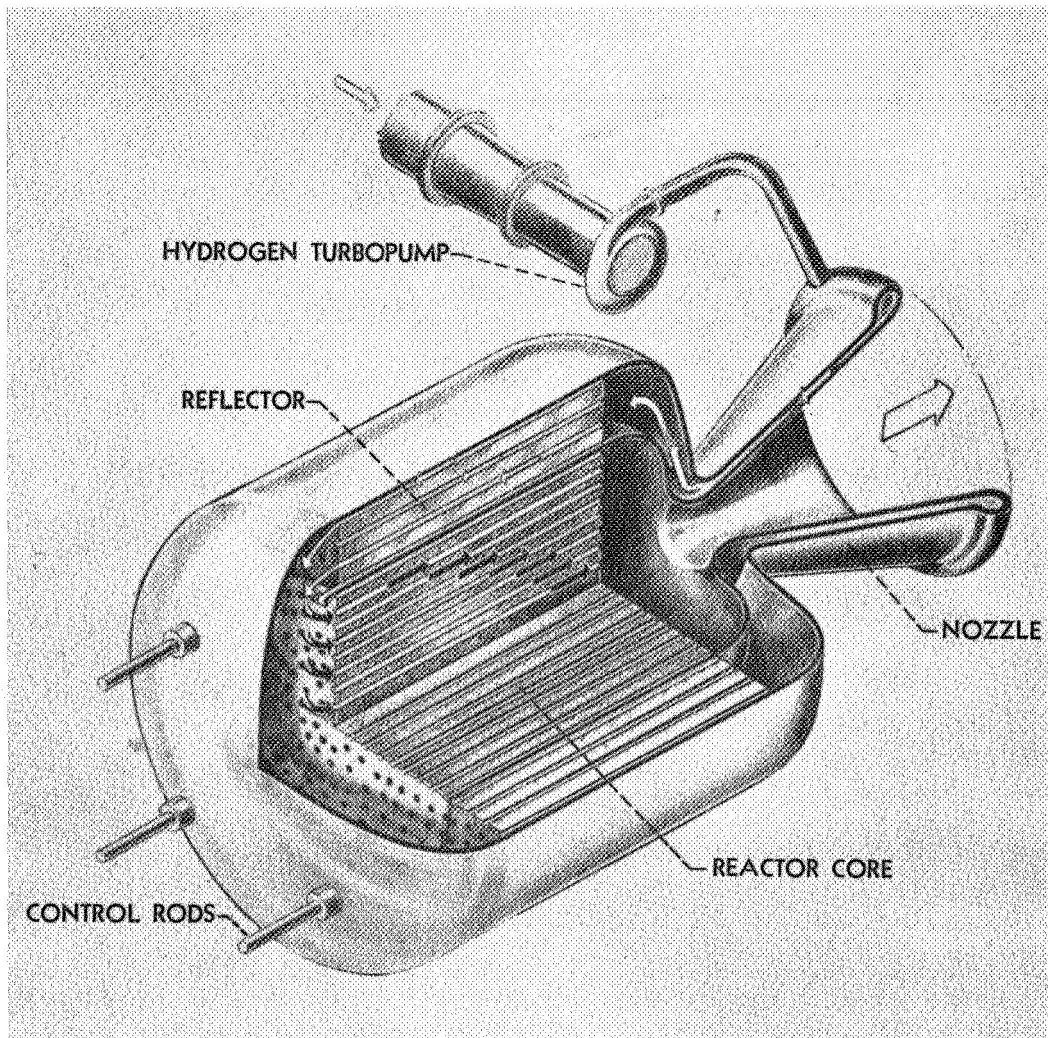


Figure 1. Cutaway Sketch of a Solid Core Nuclear Rocket Reactor
(From NASA Report SP-20, reference 13)

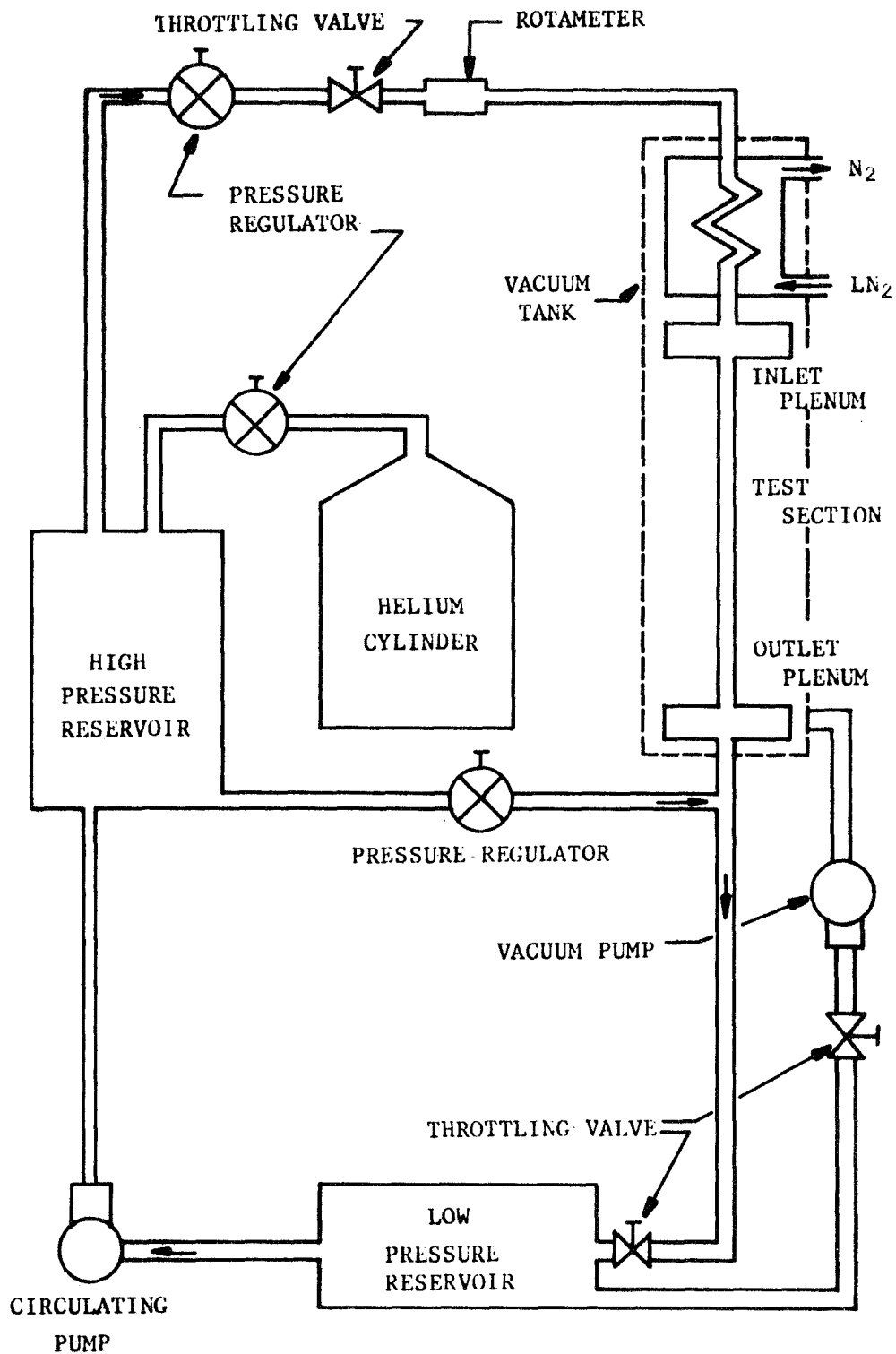


Figure 2. Flow Diagram for Experimental Apparatus

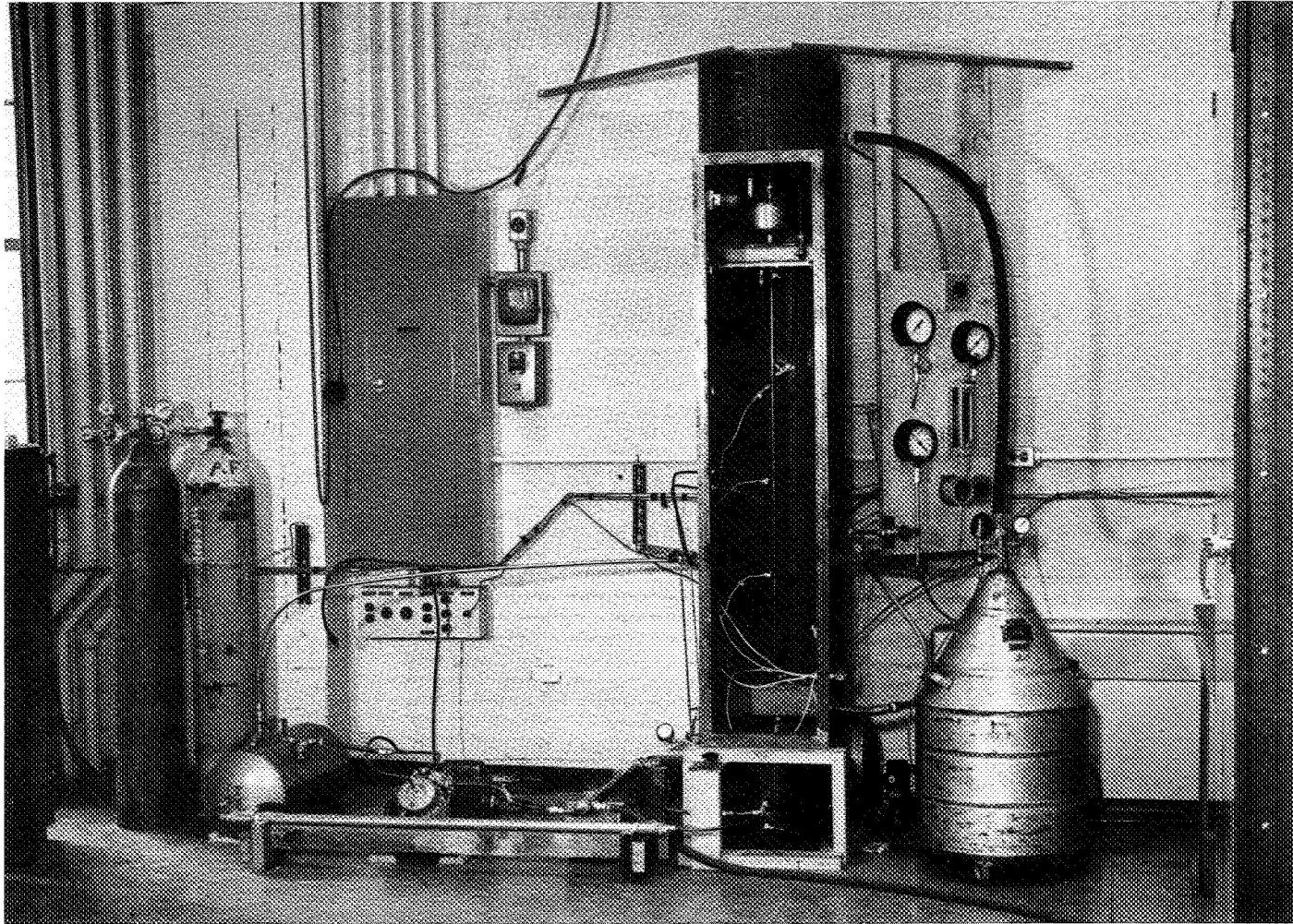


Figure 3. Photograph of Vacuum Tank and Associated Instrumentation

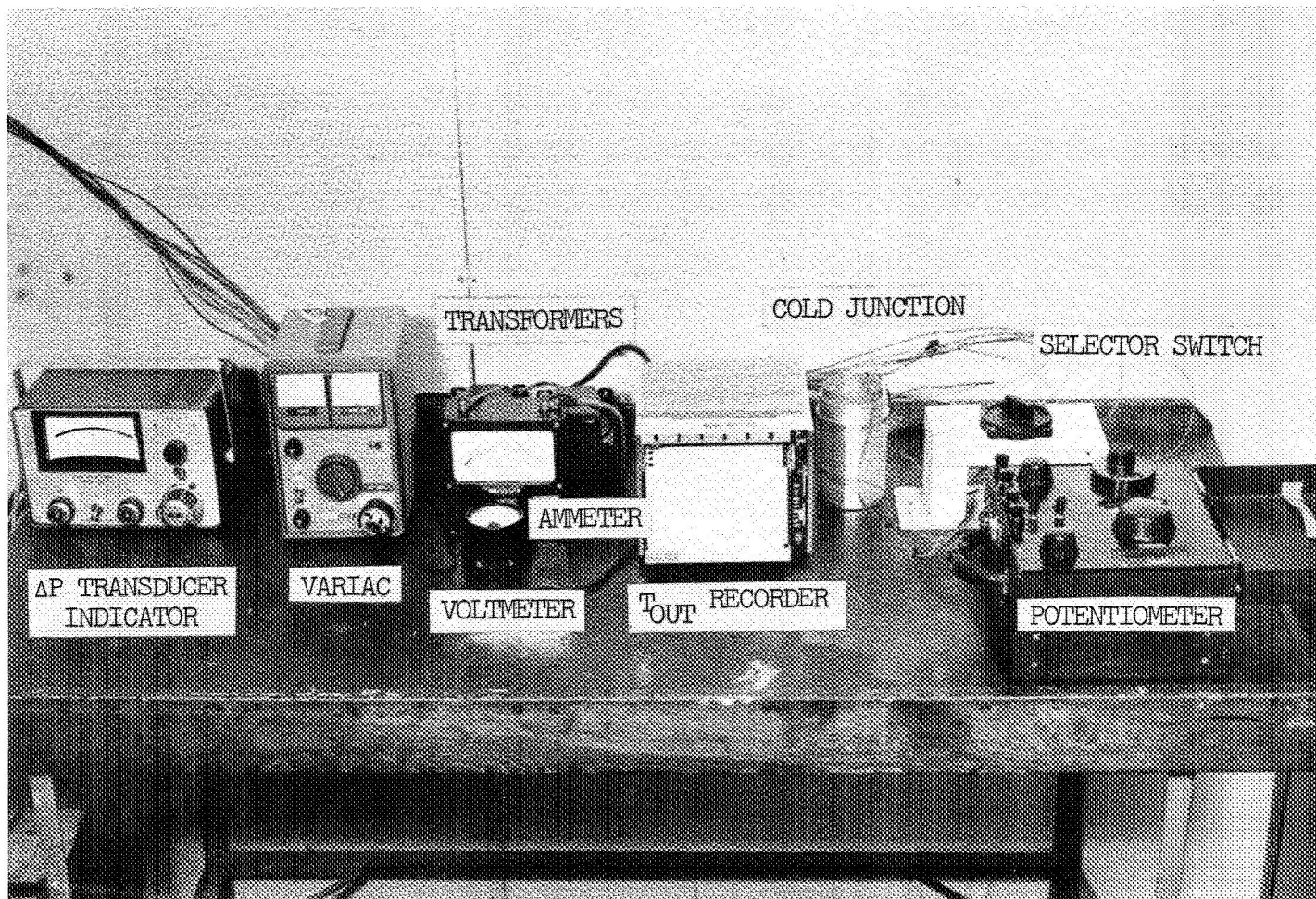


Figure 4. Instrumentation for Heating, Temperature and Δp Measurements

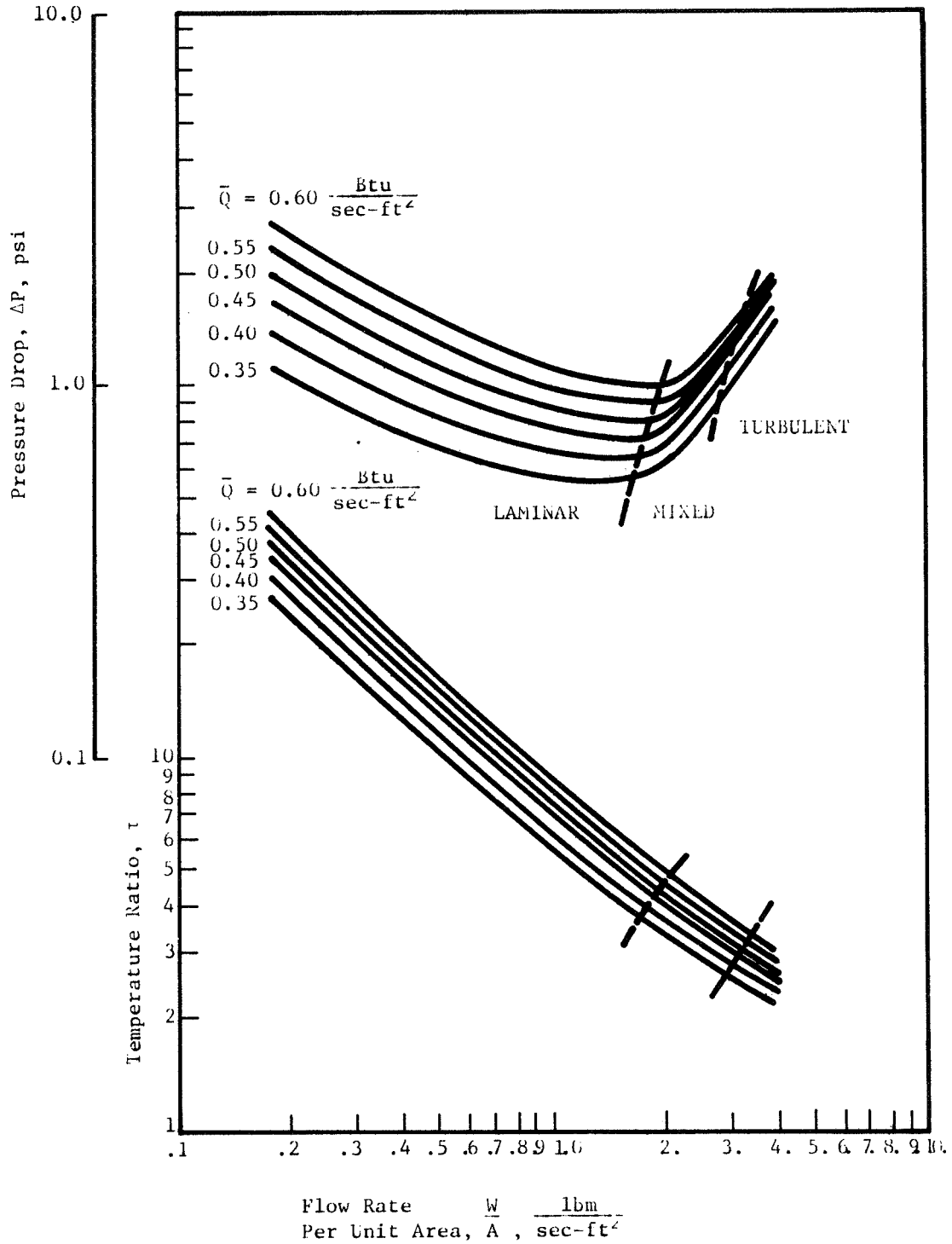


Figure 5. Theoretically Calculated Steady-State Characteristics. Helium; Inlet Pressure, 1 Psig; Inlet Temperature, 140°R, Tube Diameter, 0.094 in.; Tube Length, 4.5 Ft.

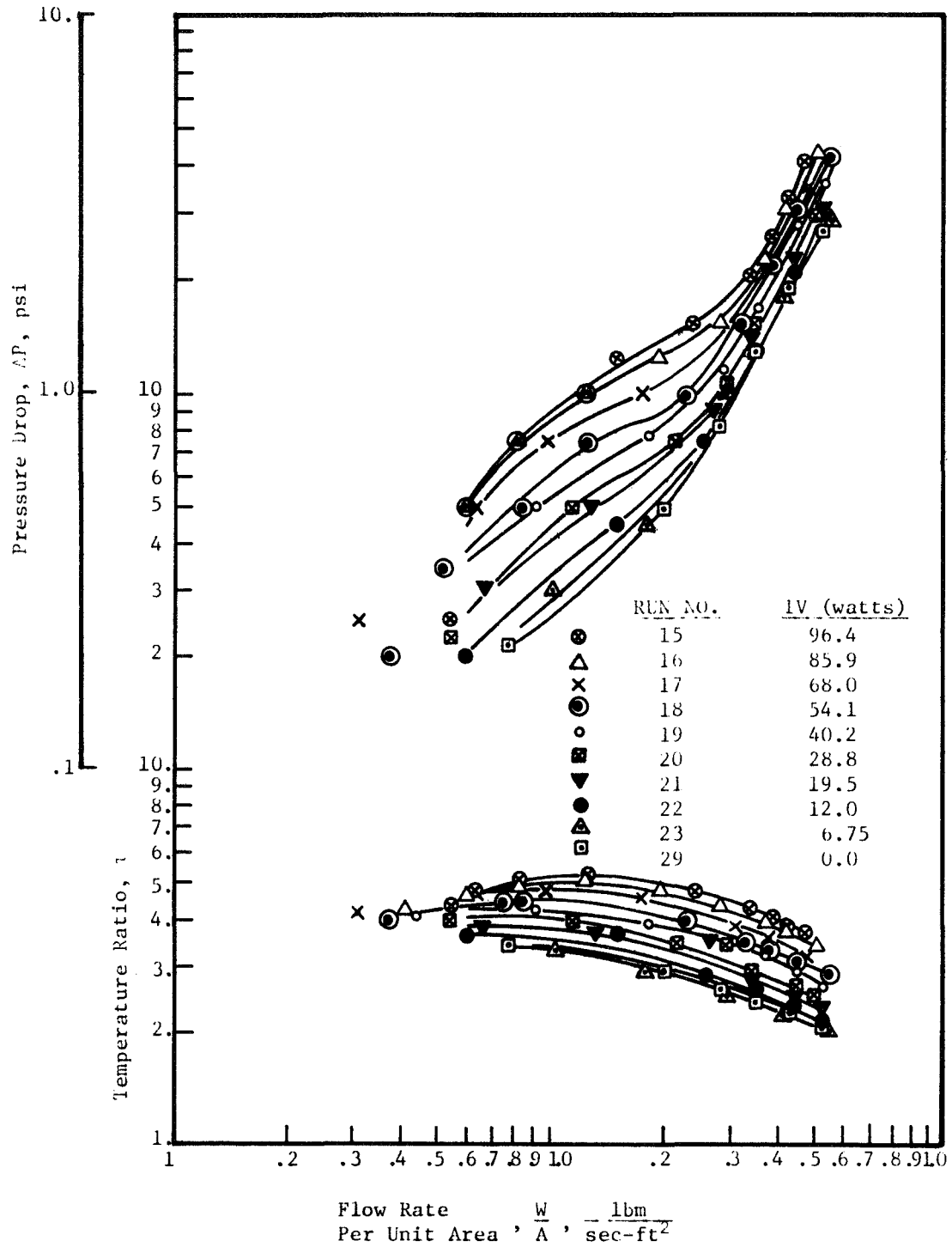


Figure 6. Experimentally Observed Steady-State Characteristics For Constant Electrical Heating helium; Inlet Pressure, 1 Psig; Inlet Temperature, 140° R Tube Diameter, 0.094 In.; Tube Length, 4.5 Ft.

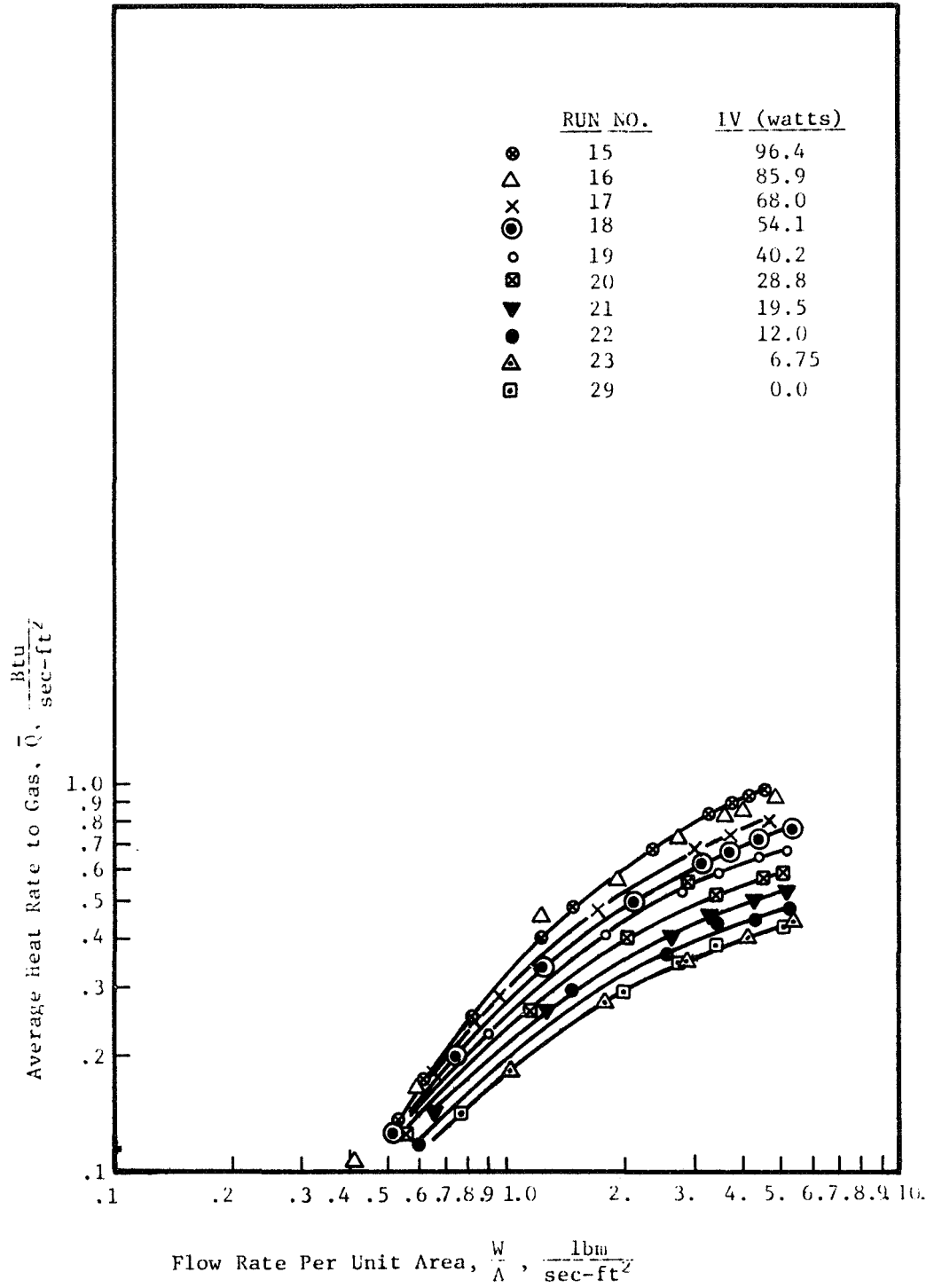


Figure 7. Calculated Heat Rate to the Gas for Constant Electrical heating

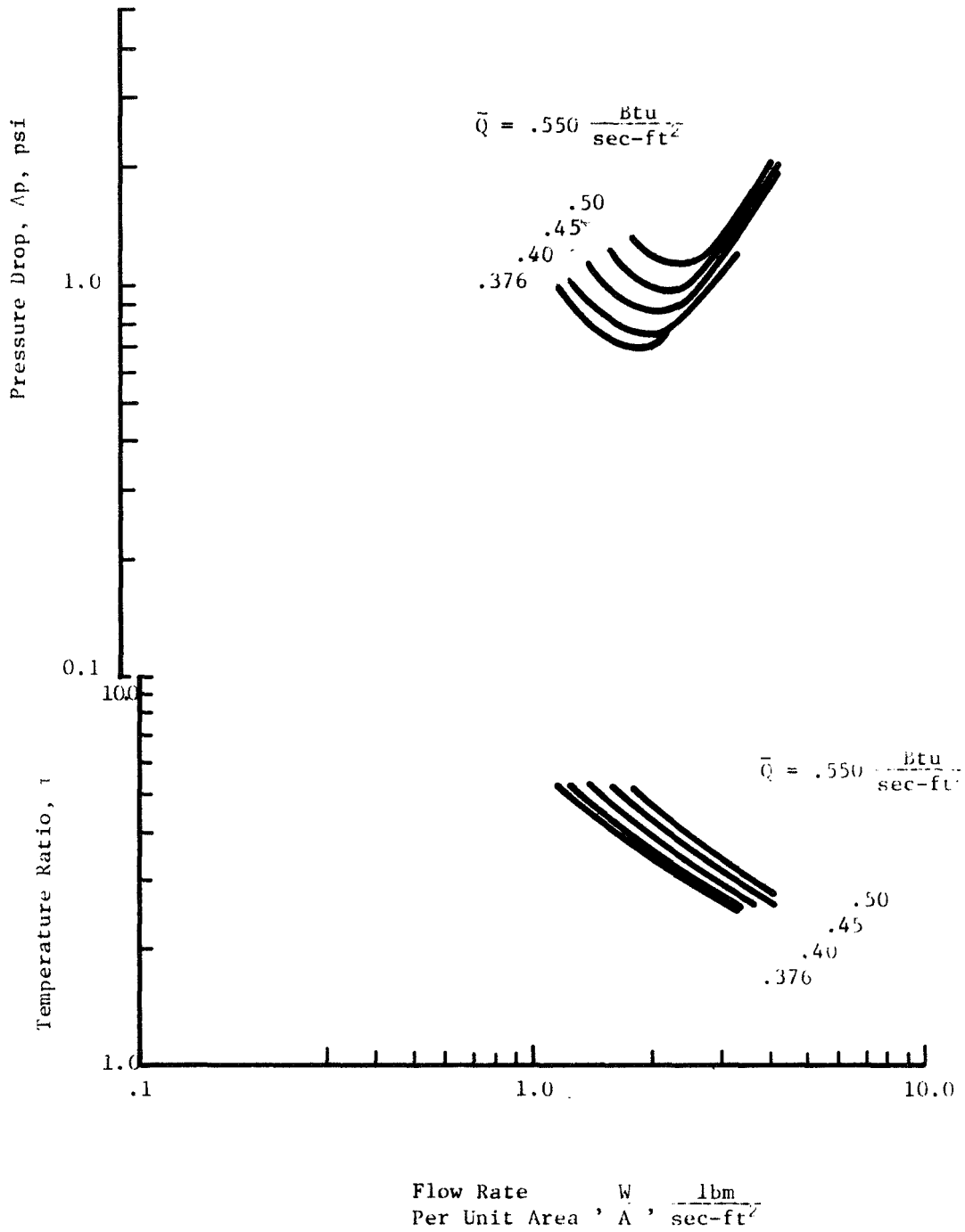


Figure 8. Experimental Steady-State Characteristics for Constant Heat Rate to the Gas Helium; Inlet Pressure, 1 psig; Inlet Temperature, 140°R; Tube Diameter, 0.094 In.; Tube Length, 4.5 Ft.

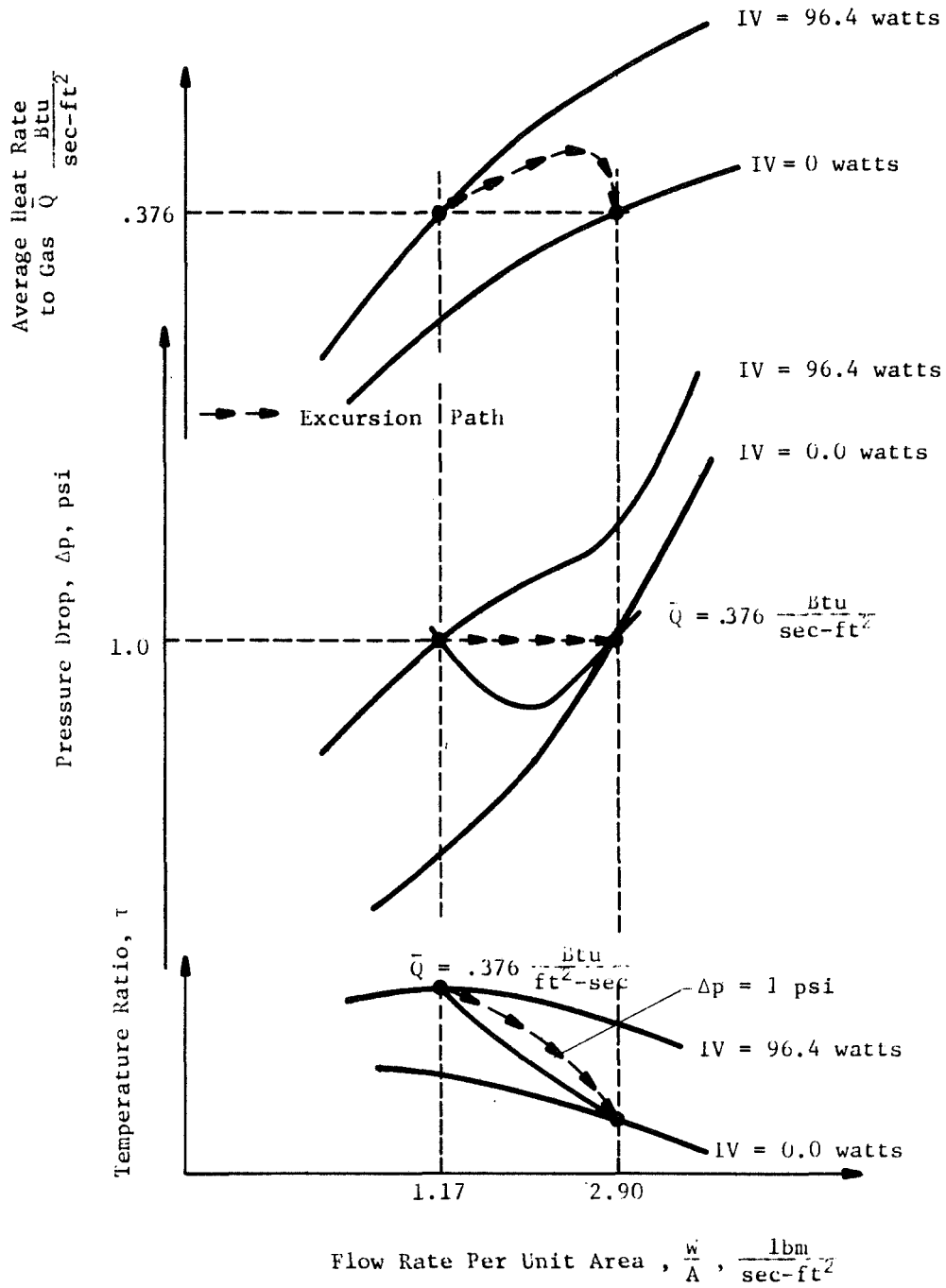


Figure 9. Schematic of Excursion Path

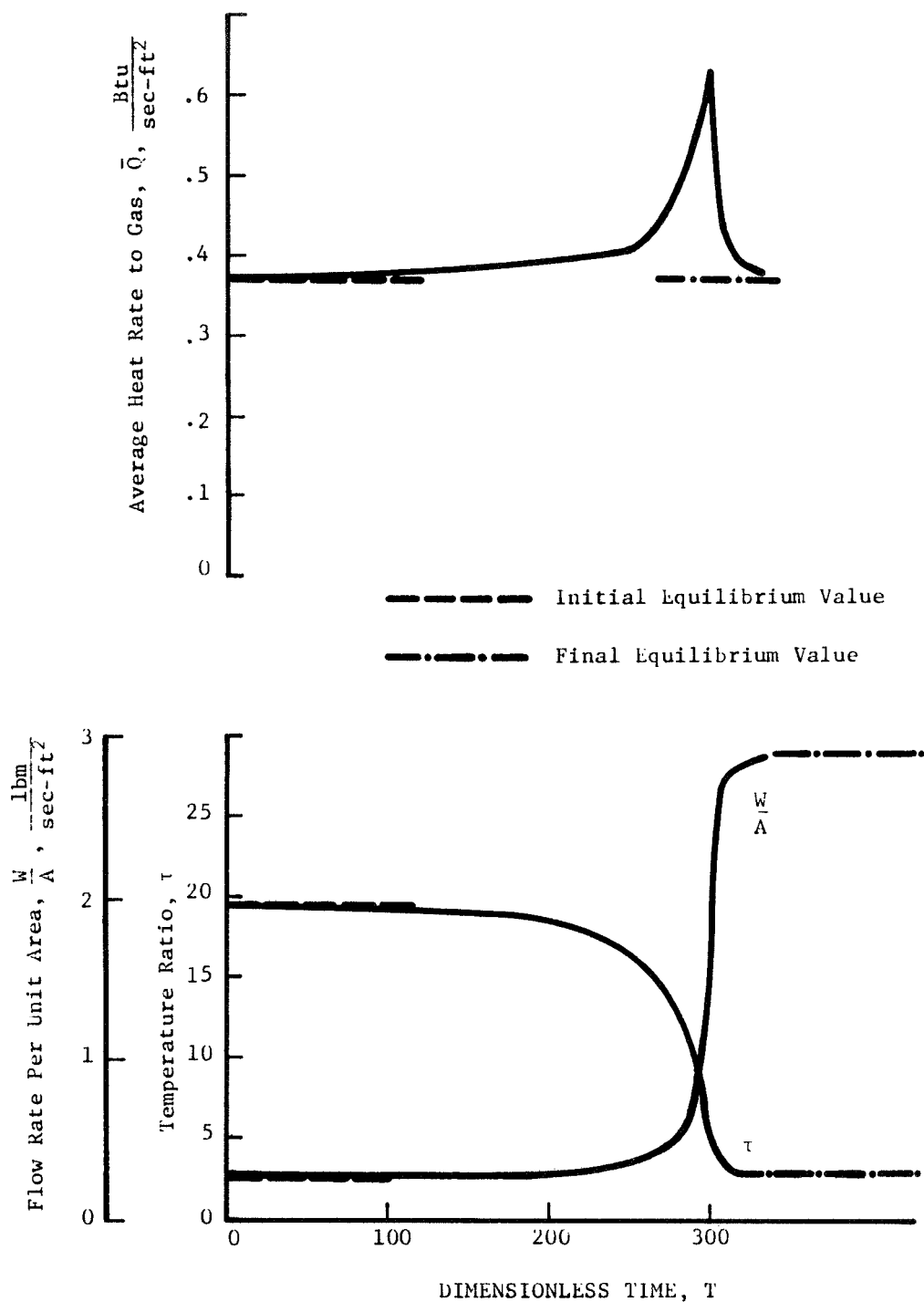


Figure 10. Excursion Characteristics Calculated From Theoretically Predicted Steady-State Characteristics ($\bar{Q}_0 = \text{constant}$)

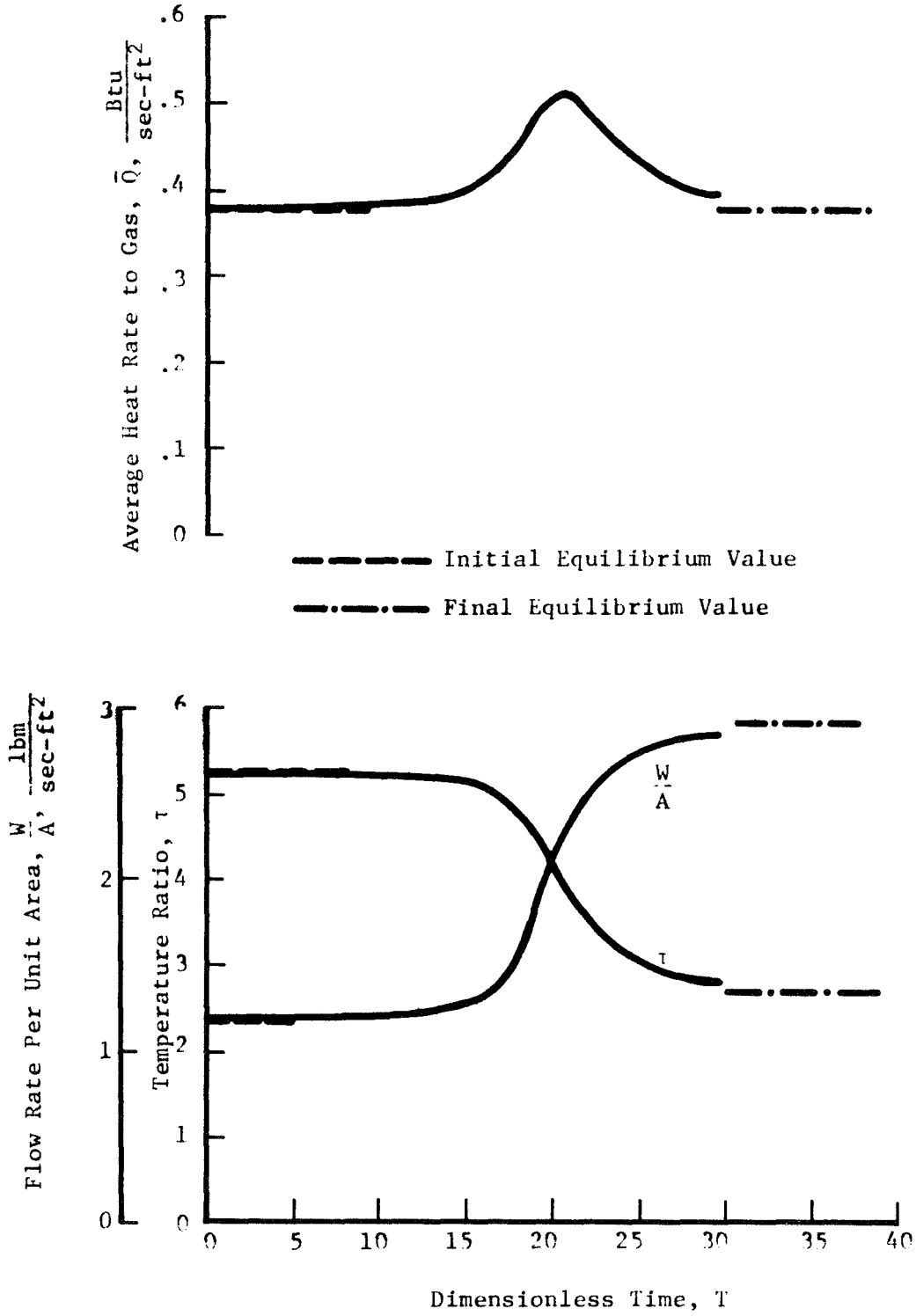


Figure 11. Excursion Characteristics Calculated From Experimentally Observed Steady-State Characteristics ($\bar{Q}_0 = \text{constant}$)

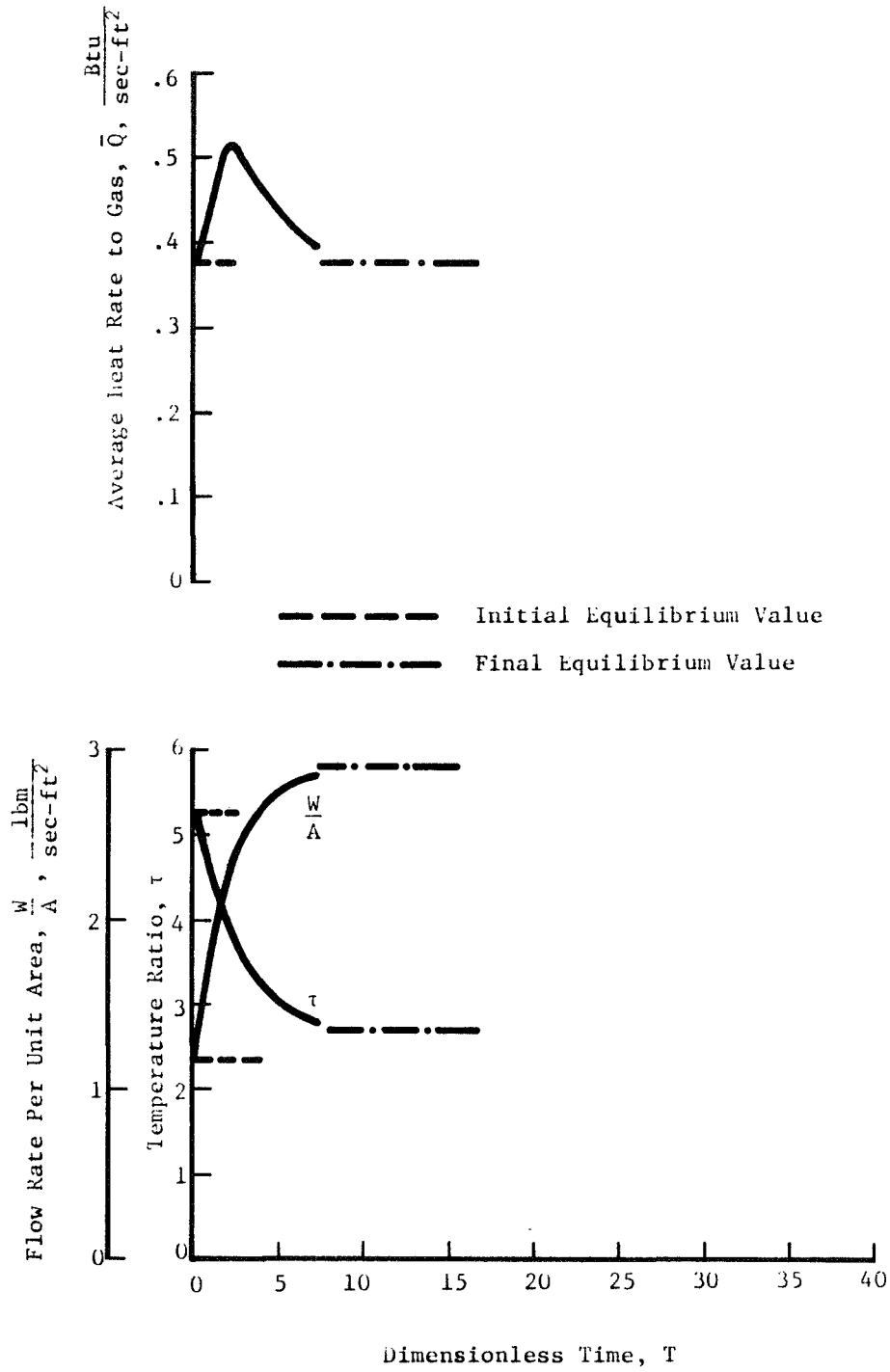


Figure 12. Excursion Characteristics Calculated From Experimentally Observed Steady-State Characteristics ($\bar{Q}_0 \neq \text{constant}$)

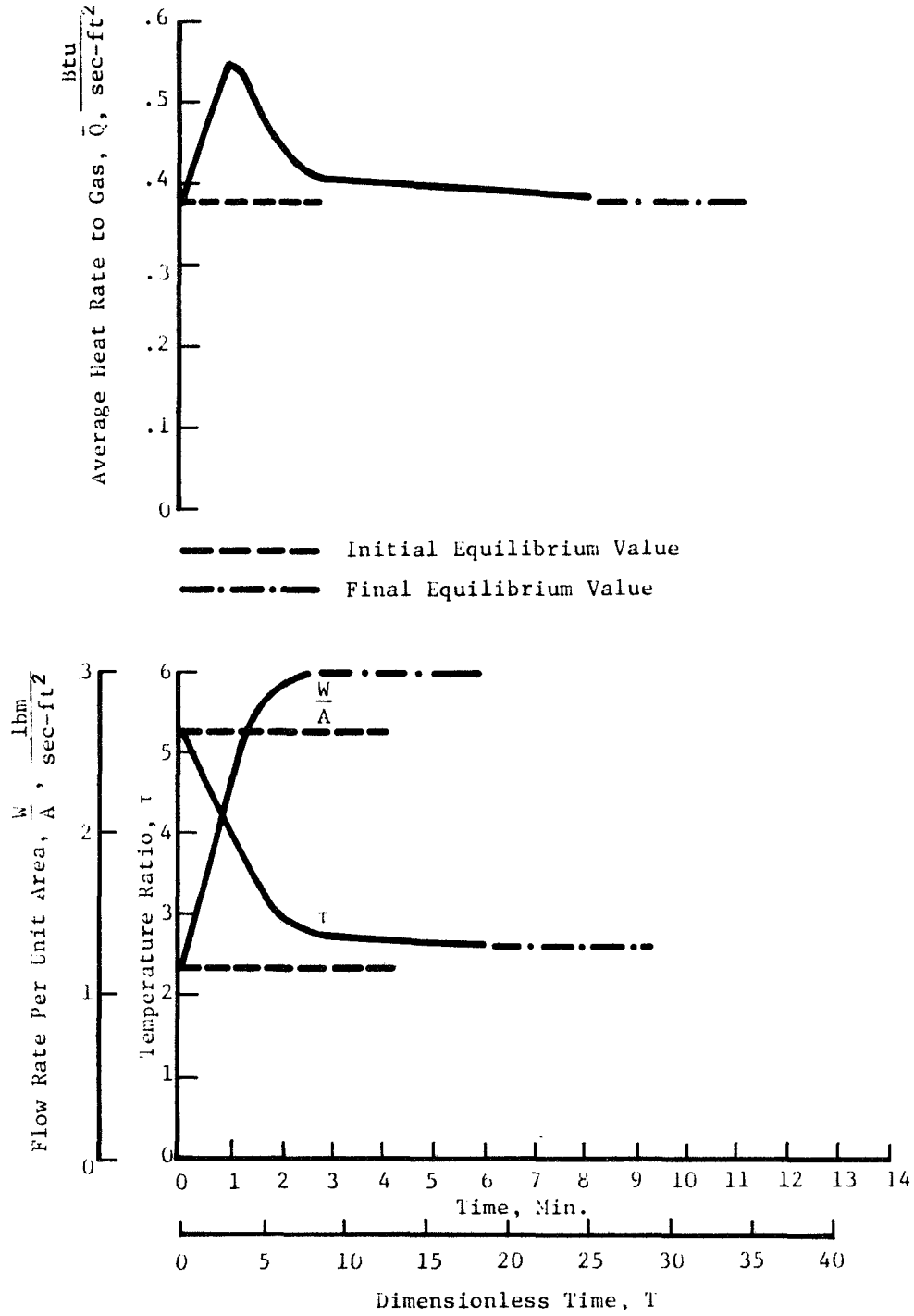


Figure 13. Experimentally Observed Excursion Characteristics

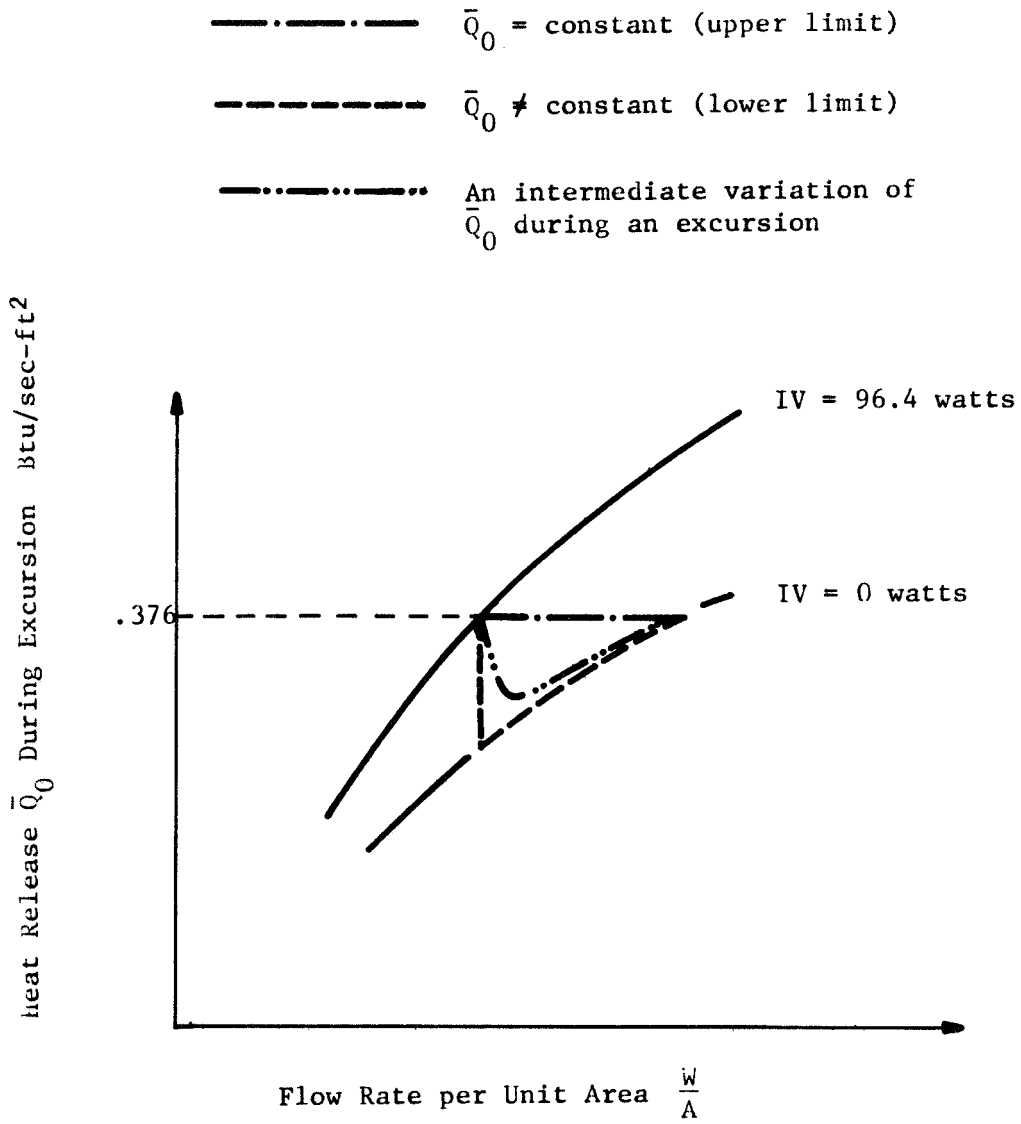


Figure 14. Possible Variation of \bar{Q}_0 During Excursion Experiment